In Vitro Prediction of Polycyclic Aromatic Hydrocarbon Bioavailability of 14 Different Incidentally Ingested Soils in Juvenile Swine

Kyle James[1, 2], Rachel E Peters[1, 2], Mark R Cave[3], Mark Wickstrom[4], and Steven D Siciliano[1*]

[1] Department of Soil Science, University of Saskatchewan, Saskatoon, Canada

[2] Toxicology Graduate Program, University of Saskatchewan, Saskatoon, Canada

[3] British Geological Survey, Nottingham, United Kingdom

[4] Veterinary Biomedical Sciences, University of Saskatchewan, Saskatoon, Canada

Title Running Head

Improving PAH bioavailability predictions

***Corresponding Author Contact Information**

Steven Siciliano

51 Campus Drive, Department of Soil Science, Agriculture Bldg

University of Saskatchewan

Saskatoon, SK, Canada, S7N 5A8

Phone: 306-966-4035. Fax: 306-966-6881

Email: steven.siciliano@usask.ca

Abstract

Predicting mammalian bioavailability of PAH mixtures from in vitro bioaccessibility results has proven to be an elusive goal. In an attempt to improve in vitro predictions of PAH soil bioavailability we investigated how energetic input influences PAH bioaccessibility by using a high and low energetic shaking method. Co-inertia analysis (COIA), and Structural Equation Modelling (SEM) were also used to examine PAH-PAH interactions during ingestion. PAH bioaccessibility was determined from 14 historically contaminated soils using the fed organic estimation of the human simulation test (FOREhST) with inclusion of a silicone rod as a sorption sink and compared to bioavailability estimates from the juvenile swine model. Shaking method significantly affected PAH bioaccessibility in the FOREhST model, with PAH desorption from the high energy FOREhST almost an order of magnitude greater compared to the low energy FOREhST. PAH-PAH interactions significantly influenced PAH bioavailability and when these interactions were used in a linear model, the model predicted benzo(a)anthracene bioavailability with an slope of 1 and r^2 of 0.66 and for benzo(a)pyrene bioavailability has a slope of 1 and r^2 of 0.65. Lastly, to confirm the effects as determined by COIA and SEM, we spiked low levels of benzo(a)anthracene into historically contaminated soils, and observed a significant increase in benzo(a)pyrene bioaccessibility. By accounting for PAH interactions, and reducing the energetics of in vitro extractions, we were able to use bioaccessibility to predict bioavailability across 14 historically contaminated soils. Our work suggests that future work on PAH bioavailability and bioaccessibility should focus on the dynamics of how the matrix of PAHs present in the soil interact with mammalian systems. Such interactions should not only include

the chemical interactions discussed here but also the interactions of PAH mixtures with mammalian uptake systems.

Introduction

Polycyclic aromatic hydrocarbons (PAHS) are carcinogenic compounds produced from incomplete combustion of organic material. Due to their relatively low solubility and vapour pressure PAHs will accumulate in soil over time and humans are exposed to PAHs through the incidental ingestion of PAH contaminated soil. The default assumption for exposure assessment is that all of the ingested PAHs have been solubilised and absorbed (i.e. 100% bioavailable) from the gastrointestinal tract, however a significant fraction of PAHs are strongly bound to soil constituents and are not released within the gastrointestinal tract.[1, 2]

PAH bioavailability from soil is estimated by monitoring uptake of PAHs into the bloodstream of a model organism, e.g. mice, swine or rats. Animals should, ethically, not be used for routine site assessments and thus, substantial effort has gone into developing in vitro bioaccessibility models to predict bioavailability. Current models for organic contaminants include Physiologically Based Extraction Test (PBET),[3-5] Colon-extended PBET,[6] Fed Organic Estimation human Simulation Test (FOREhST),[2, 7] Relative Bioaccessibility Leaching Procedure (RBALP),[8] as well as simulation of the human intestinal microbial ecosystem (SHIME).[7] To ensure that hydrophobic organic contaminant soil release is not limited to the compound solubility for the simulated intestinal fluids, a sorption sink such as C18 membranes, [8, 9] tenax beads,[5] ethyl vinyl acetate thin films,[10] and silicone rods[11] are incorporated into the models. These models can often predict the bioavailability of different PAHs within a soil,[1] but typically are not successful in estimating bioavailability between soils.

Juhasz et al.[12] noted that maximizing estimated bioaccessibility is not necessarily the most conservative measure of bioavailability (ie. bioaccessibility can be less that bioavailability).

63 Bioaccessibility is dependent upon the desorption conditions within the in vitro model, i.e.
64 shaking method, temperature, desorption media, and desorption time.[13, 14] PAH release in *in*
65 *vitro* models is linked to the activation energy of the desorption process[15] as well as organic
66 matter composition.[16, 17] PAHs bind to either amorphous organic matter with non-competitive
67 fast desorption kinetics or to carbonaceous geosorbents with competitive slow desorption
68 kinetics.[18] A typical soil has both amorphous and carbonaceous geosorbents and regardless of
69 carbon type, longer desorption times typically lead to greater desorption.[14] The RBALP model,
70 which utilizes end-over-end rotation, can be coupled with a lipid sink and leads to high PAH
71 release from soil.[8] Under such conditions, PAH bioaccessibility closely tracks PAH soil
72 concentration but not PAH bioavailability[8]. In vitro models that use reduced energetic input,
73 such as the TIM model,[19] will result in lower PAH release and perhaps this release is linked more
74 closely to bioavailability. Our rationale for this hypothesis is that the current generation of in
75 vitro models assumes that maximizing bioaccessibility will better predict bioavailability. While
76 possible, our experience is that these *in vitro* approaches closely mirror chemical activity but
77 not bioavailability. Hence, we modified the existing FOREhST model to reduce energetic inputs
78 during extraction and compared this release to in vivo bioavailability results.
79 PAHs are present as mixtures and depending on the source of the PAHs, e.g. pyrogenic,
80 petrogenic, etc., the relative ratios of each PAH will change.[20] The nature of this PAH mixture is
81 a major factor influencing PAH bioaccessibility/bioavailability.[21] It is thought that these mixture
82 effects occur because PAHs interact with other PAHs and influence their partitioning behavior.
83 For example, phenanthrene solubility in various surfactants was enhanced in the presence of
84 naphthalene yet reduced in the presence of pyrene.[22] Benzo(a)pyrene concentrations in gut

fluids increased in the presence of cholesterol (137%), phenanthrene (154%), lecithin (140%) and hexadeconal (232%).[23] Given that PAHs interact with each other, it is likely that linking PAH bioaccessibility to PAH bioavailability between soils requires that we explicitly link the matrices of PAH accessibility to PAH bioavailability.

Co-inertia analysis is statistical method developed to study the common structure of multiple sets of paired data.[24] Co-inertia analysis is a non-directional approach to identify individual variables within each matrix that influence the other corresponding matrix and is well suited to situations where the number of samples is low relative to the number of predictor variables. Here we use co-inertia to identify key PAHs in the bioaccessibility matrix that are influencing other PAHs in the bioavailability matrix. However, co-inertia analysis is largely an exploratory statistical approach, and thus we tested if these PAHs were significantly influencing bioavailability using structural equation modelling. Structural equation modelling (SEM) is well suited for assessing a hypothesis that links collinear variables in a causal network to predict a dependent variable.[25] Furthermore, unlike multiple regression approach, structural equation modelling explicitly accounts for collinearity and thus, allows one to estimate, not only the significance, but the strength of a relationship linking predictors (such as the bioaccessibility of single PAHs) to the bioavailability of a PAH.

Our goal here was to combine the concepts of bioaccessibility and bioavailability as outlined by Juhasz et al.[12] and Reichenberg and Mayer[13], with explicit multivariate predictive approaches, to develop a numerical prediction of bioavailability based on a widely adopted bioaccessibility protocol. We then evaluated the robustness of this prediction by spiking PAHs

into water or soil and confirming that the drivers identified by the multivariate approaches were indeed occurring in in vitro settings.

Materials and Methods

Soils

A total of 14 PAH contaminated soils have been collected from the United Kingdom (n = 12) and Sweden (n =2) as previously described by Cave et al.[7] and James et al.[8] Soil pH, organic carbon, and particle size were analyzed as previously described by Siciliano et al.[26]

Sorptive sink

Silicone rods, poly(dimethylsiloxane) (PDMS), are chosen to act as a PAH sorption sink as they have established partitioning properties for PAHs and have been previously used for in vitro bioaccessibility testing.[4, 21] The silicone rod (Altec, Cornwall, United Kingdom) has a diameter of 2.87-3.13 with a mass of 8.0 g m^{-3}. To prepare the silicone rods for experimental use, the procedures of Gouliarmou et al.[11] are followed, where the silicone was cleaned by soaking once overnight with ethylacetate, three times overnight with methanol, 3 times overnight with acetone, and 4 times overnight with Milli-Q water.

FOREhST

Shaking Method / Energetic input

To investigate the effects of energetic inputs two shaking methods were employed. The first is the standard high energy FOREhST where 125 mL glass bottles are rotated 30 rpm end-over-end inside of a water bath held at 37°C. The second method uses a less aggressive process to create a massaging motion that utilizes 2 – 1.5” rotating spherical balls moving back and forth horizontally (Supporting Information Figure S1). Modified polytetrafluoroethylene (PTFE)

bags (5”x4”- 5.0 Mil thick, Welch Fluorocarbon, Dover, New Hampshire) are used with this lower energy method, as their inherent flexibility allows for a massaging technique. In the low energy method, the FOREhST fluids are warmed up to 37°C prior to use and cool down to 28-32°C after 2 hours.

The FOREhST model described here follows the detailed procedures of Cave et al[7]. The FOREhST model is an adaption of the fed state methods developed by the RIVM - The Netherlands National Institute for Public Health and the Environment[27] and is intended for organic contaminants.[7] The fed state is the most conservative estimate of bioaccessibility for organic contaminants[28]. The compartments of the FOREhST model are saliva, gastric and intestinal, which consist of simulated fluids modeled to the physiochemical conditions present at each stage.

To each experimental unit, 0.3 g of contaminated soil is added, followed by approximately 0.8 g of HIPP creamy porridge™, 2.45 mL of deionized water, 50 µL sunflower oil, and 1 m silicone rod. Saliva fluid, 4.5 mL, is added to each unit and shaken for 5 min. Afterwards, 9 mL of gastric fluid is added and incubated for 2 hours. Finally, 9 mL of duodenal fluid and 4.5 mL of bile fluid were added, followed by an additional 2 hour incubation.

Post incubation, silicone rods are removed from the extraction units, washed with Milli-Q water and gently dried with lint free tissue paper. PAHs are extracted by soaking silicone rods in approximately 50 mL of acetone twice for 24 hours.[11] The 100 mL acetone was evaporated using nitrogen gas to near dryness, re-constituted into 1.8 mL of acetonitrile into 2 mL HPLC vials and stored at -20°C until analysis.

Co-Solubility Experiments

150 Phenanthrene (96%), pyrene (98%), and benzo(k)fluoranthene (99%) were obtained
151 from Sigma Aldrich, while benzo(a)pyrene was obtained from MRI Global. Bioaccessibility
152 experiments were conducted using de-ionized water and bile fluid. Bile fluid was prepared by
153 dissolving 12.5 g L^{-1} bile and 6 g L^{-1} $NaHCO_3^-$ into de-ionized water. To each experimental unit, 1
154 m of silicone rod is inserted into a 125 mL amber glass jar. To the jar, approximately 35 ± 5 mg
155 of PAH is added, followed by 100 mL of either de-ionized water or bile fluid. Notably the
156 solubility limits of these PAHs in water is less than 1.2 mg L^{-1}.[29] The amber jar was then gently
157 shaken on a horizontal shaker for 4 hours, the time was chosen to be representative of the
158 gastric and intestinal transit time of the FOREhST model.

159 **Low energy FOREhST spiking**

160 The low energy FOREhST was repeated for five soils and spiked with benzo(a)anthracene
161 (99%, Sigma-Aldrich) or fluoranthene (99%, Sigma-Aldrich) dissolved in 100 µL of acetonitrile.
162 The spiking consisted of five concentrations for each benzo(a)anthracene and fluoranthene.
163 Soils were also spiked with 100 µL of clean acetonitrile as a solvent control. Spiking solution
164 was added directly to the FOREhST media, in the mixture containing soil, water, food, saliva and
165 silicone rod.

166 **In vivo Swine Oral Bioavailability**

167 The oral bioavailability and area under the plasma concentration curve over a 48 hour
168 time period (AUC48) of PAHs to swine has been previously reported by James et al.[1]

169 **HPLC analysis**

170 PAHs were analyzed using an Agilent 1260 Infinity high pressure liquid chromatography
171 coupled with fluorescence detection (HPLC-FD).[30] A 10 µL aliquot was injected onto an Agilent

PAH Pursuit Column (3 µm particle size, 2mm internal diameter). The mobile phase consists of acetonitrile and water with a flow rate of 1.5 mL min^{-}. The acetonitrile:water gradient at the start of the run was 60:40 and gradually increases to 95:5 at 20 min, this gradient is held constant until the end of the run at 25 min. The column temperature is held constant at 25°C for the duration of the run. The fluorescence detector utilizes an excitation wavelength of 260 nm and four emission wavelengths of 350, 420, 440 and 500 nm. Detection limits for anthracene is 0.70 pg µL, fluoranthene is 1.71 pg µL, pyrene is 0.43 pg µL, benzo(a)anthracene is 2.45 pg µL, chrysene is 5.27 pg µL, benzo(b)fluoranthene is 5.58, benzo(k)fluoranthene is 2.77 pg µL, benzo(a)pyrene is 13.02 pg µL, dibenzo(a,h)- anthracene is 7.79 pg µL, benzo(g,h,i)perylene is 1.78 pg µL, and indeno(1,2,3-cd)pyrene is 1.80 pg µL.

Quality Assurance and Control

To quantify the PAH recovery from soil, a sand matrix spike was added every 10 samples and the average recovery ranges from 77% to 94% with a standard deviation of 12%. Benzo(b)chrysene is present at very low concentrations in all soils and was used as an internal standard and the recovery ranged between 90% to 110% with a standard deviation of 11%. For the in vitro digestors, a blank sample (no soil) is included every 8 samples. Average blank samples recovered a range of 0 to 120 pg from the high energy FOREhST, 110 to 810 pg from the low energy FOREhST, and 0 to 120 pg from the low energy FOREhST spiked with acetonitrile. Residual PAHs adhering to PTFE bags range from 0 to 1400 pg.

Statistical Analysis

Co-Inertia Modeling

193 Co-Inertia analysis (COIA) was performed using R software[31] and the "ade4"[32] package.
194 Co-inertia analysis developed by Deledec and Chessel[33] was reviewed by Thioulouse[24] and
195 compared with canonical correspondence analysis by Dray et al.[34] Co-inertia analysis is an
196 alternative method to canonical correspondence analysis when number of samples is low
197 relative to the number of predictor variables. Co-inertia analysis investigates the common
198 structure of paired data tables by maximizing the covariance of the row scores between the
199 tables. High co-inertia occurs when simultaneously high values (or inverse) occur in both
200 tables, whereas low co-inertia occurs either when they vary independently or they do not vary.
201 Thus, high scores indicate that parameters, such as a specific PAH, are concordant between two
202 sets of data tables, whereas low scores indicate that these specific PAHs are discordant (or in
203 other words, PAHs behaving dissimilarly between the two data tables, which in this case would
204 be the soil concentration data table consisting of different soils versus different PAHs
205 bioaccessibility compared to the data table of different PAH's bioavailability).
206 PAHs have the ability to interact with each other and affect the solubility of each other,
207 and in the environment PAHs are present as mixtures. When investigating the bioavailability of
208 PAHs it is likely that the bioavailability of one PAH will affect the bioavailability of another, the
209 same can be said for bioaccessibility; however the goal is to use bioaccessibility to predict
210 bioavailability. In addition to bioaccessibility, other environmental variables such as soil PAH
211 concentration, organic matter, soil texture, and soil metal concentrations may be used as
212 predictive variables of PAH bioavailability. In one table there is bioavailability of individual
213 PAHs, in columns, by soil samples, in rows. In another table there are the predictor variables,

214 including bioaccessibility of individual PAHs, as well as PAH concentration , organic matter, soil
215 texture, and soil metal concentrations, in columns, by the same soil samples in rows.
216 The two data sets were first studied separately with Principal Components Analysis
217 (PCA), and eventually analyzed as PCA-PCA COIA. In a PCA-PCA COIA, the two PCA's on the
218 original two data sets reduces their dimensionalities by selecting the dominant components
219 (axes). COIA uses the principle components from each data set and merges the complied data
220 into a new multidimensional space such that the covariance between axes of each data set is
221 maximized. The data tables are not transformed prior to analysis.
222 **Model Selection**
223 Co-inertia analysis provides the primary components for predicting PAH bioavailability.
224 Using the results from co-inertia analysis, a general linear model is constructed consisting of the
225 dependent variable, $AUC48_{PAH}$, being regressed on by $FOREhST_{PAH}$, $[soil]_{PAH}$, and the top five
226 variables as given by co-inertia analysis. Non-significant variables are then stepwise removed
227 using the "stepAIC" function from the "MASS" package[35] with R software[31] until the best final
228 model is chosen. The "stepAIC" function is combined with an anova to examine significant
229 differences between model fits based on Akaike Information Criterion (AIC). Model residuals
230 are plotted against predicted values and visually inspected as per Osborne et al.[36] to ensure
231 homoscedasticity.
232 **Structure equation modelling**
233 Structure equation modelling was performed using R software[31] with the additional
234 "laavan"[37] package. SEM is a statistical method akin to path analysis which allows for testing of
235 hypotheses were the relationship is confounded by many variables inter-correlated. The

application of SEM is to determine the relative strength of the coefficient that each predictor variable has on the dependent variable in the presence of collinearity. After removing non-significant variables, SEM is used to account for collinearity between variables and to determine the path coefficients. The structure equation model is built similarly as outlined by James et al.[1], where there is a high degree of collinearity between predictor variables, such as between bioaccessible FOREhST PAHs, they are set to co-vary. Where one predictor variable predicts another, such as total organic carbon predicting soil PAH concentration, the model reads PAH soil concentration is regressed on by total organic carbon. Finally, each predictor variable is included as a direct cause of $AUC48_{PAH}$. A detailed SEM diagram is available in the supporting information (Supporting Information Figure S6)

Results

Bioaccessibility

In the standard high energy FOREhST model the PAH release correlates moderately to strongly (r^2 between 0.43-0.62) with soil concentration (Figure 1), whereas no correlation was found between the low energy FOREhST and soil concentration (Supporting Information Figure S2). The average bioaccessibilty (mean ± standard deviation in parentheses) from the high energy FOREhST was 23% (8.0 ± 9.5 μg) for benzo(a)anthracene, 29% (9.2 ± 8.1 μg) for chrysene, 20% (11 ± 7.9 μg) for benzo(b)fluoranthene, 21% (4.4 ± 2.7 μg) for benzo(k)fluoranthene, and 13% (5.6 ± 5.8 μg) for benzo(a)pyrene while the average bioavailability from the low energy FOREhST was 3.7% (0.76 ± 0.65 μg) for benzo(a)anthracene, 5.0% (1.2 ± 0.96 μg) for chrysene, 3.0% (0.99 ± 0.58 μg) for benzo(b)fluoranthene, 3.4% (0.38 ± 0.24 μg) for benzo(k)fluoranthene, 1.6% (0.41 ± 0.30 μg) for benzo(a)pyrene.

Bioaccessibility and Bioavailability

Between soils, neither the low or high energy FOREhST model predicts in vivo AUC48 juvenile swine exposure for individual PAHs (Supporting Information Figure S3). However, within a soil, both the low and high energy FOREhST predict in vivo AUC48 exposure between PAHs (Figure 2). Within a soil, desorption of PAHs is predictable likely due to the physiochemical properties of the PAH, as such they desorb from soil at a relative rate, however between soils, the PAH release cannot be predicted. The low energy FOREhST predicts exposure between PAHs with a slope of 1.9 ($r^2 = 0.64$, $p < 0.01$) while the high energy FOREhST predicts exposure between PAHs with a slope of 0.34 ($r^2 = 0.81$, $p < 0.005$). Notably, the energetic input does not appear to affect all PAHs equally. In Figure 2, the high energy FOREhST does not accurately predict anthracene, fluoranthene and pyrene AUC48, however the only outlier in the low energy FOREhST model is fluoranthene.

Co-Inertia Analysis

The PCA on PAH bioavailability reduces the data set to six principal components that explain 94.9% of the variance while the PCA on predictor variables (PAH bioaccessibility, PAH soil concentration, and soil properties) reduces the data set to five principle components that explain 90.2% of the variance (Supporting Information Table S3 and S4). COIA indicates that the primary variables predicting PAH in vivo exposure are FOREhST release of chrysene, fluoranthene, anthracene, and benzo(a)anthracene, followed by soil arsenic concentration, and then FOREhST release of pyrene and benzo(k)fluoranthrene. The relative rankings of the individual predictor variables are determined using the 'Strength' of the predictive vector as determined by the canonical weights of COIA (Supporting Information, Table S5).

Model selection

The top five variables given from COIA predicting PAH in vivo exposure are FOREhST release of chrysene, fluoranthene, anthracene, and benzo(a)anthracene, followed by soil arsenic concentration. We evaluated these variables as well as soil concentration and FOREhST release of the individual PAH (either benzo(a)anthracene or benzo(a)pyrene) for their ability to predict bioavailability. After removing non-significant predictor variables, the most parsimonious model for benzo(a)anthracene AUC48 includes FOREhST release of benzo(a)anthracene, fluoranthene and chrysene, while the most parsimonious model for benzo(a)pyrene AUC48 includes FOREhST release of benzo(a)pyrene and benzo(a)anthracene (Figure 3). COIA does not evaluate information criterion and thus, will identify multiple predictors, whereas stepwise regression eliminates predictors based on their information content. When combining significant predictor variables into a general linear model ($B(a)A_{AUC48} \sim B(a)A_{FOR} + FLUO_{FOR} + CHR_{FOR}$), the predicted AUC48 values were compared to observed AUC48 resulting in a slope of 1.0, r^2 of 0.66, and $p < 0.0005$. For benzo(a)pyrene, the general linear model predicts observed AUC48 with a slope of 1.0, r^2 of 0.65, and $p < 0.0005$.

Structure Equation Modelling

Our hypothesized causal network linking bioaccessibility to bioavailability was congruent ($P = 0.11$ for benzo(a)anthracene and $P = 0.13$ for benzo(a)pyrene) with the data (Supporting Information Table S6). A non-significant P value for a SEM indicates the likelihood that a completely random models fits the data better than the hypothesized causal network. Other SEM fit values, e.g. CFI and RMSE, all indicate that the SEM represented the data reasonably well. A diagram detailing the specific relationship of SEM parameters is found in supporting

information (Supporting Information Figure S6). Only, PAH bioaccessibility and not soil organic carbon content were significant predictors of bioavailability (Supporting Information Table S5). The standardized coefficients, used for comparing within a model, predicting benzo(a)anthracene AUC48 given by structure equation modelling are -1.8 for FOREhST benzo(a)anthracene, -0.29 for FOREhST chrysene, and 2.5 for FOREhST fluoranthene. The standardized coefficients predicting benzo(a)pyrene AUC48 are -0.56 for FOREhST benzo(a)pyrene and 1.0 for FOREhST benzo(a)anthracene. The SEM coefficients suggest that benzo(a)anthracene and fluoranthene counter-act each other in predicting benzo(a)anthracene bioavailability. In contrast, benzo(a)anthracene and benzo(a)pyrene counter-act each other in predicting benzo(a)pyrene bioavailability

Co-solubility

In the absence of soil (i.e. only water or bile), PAHs significantly decreased the bioaccessibility of other PAHs. The amount of benzo(a)pyrene solubilized in 100 mL of de-ionized water was 94 ± 14 μg (mean ±SE), was reduced to 39 ± 15 μg in the presence of phenanthrene, significantly ($p<0.05$) reduced to 15 ± 4.8 μg in the presence of phenanthrene and pyrene, and 13 ± 6.1 μg in the presence of phenanthrene, pyrene and benzo(k)fluoranthrene (Figure 4). The amount of bioaccessibile benzo(a)pyrene in 100 mL of simulated bile fluid was 36 ± 17 μg, and was significantly ($p<0.05$) reduced to 8.0 ± 2.5 μg in the presence of phenanthrene, 1.3 ± 2.1 μg in the presence of phenanthrene and pyrene, and 8.1 ± 2.1 μg in the presence of phenanthrene, pyrene and benzo(k)fluoranthrene (Figure 4).

Low-Energy FOREhST of Spiked Field Contaminated Soils

323 In contrast to the results in water and bile, PAH interactions in the presence of soil can
324 increase the bioaccessibility of other PAHs. Benzo(a)anthracene was spiked into the low energy
325 FOREhST model at 0, 0.38, 0.75, 1.5, 3.0 and 6.0 μg, resulting in a significant increase ($p < 0.05$)
326 in the amount of benzo(a)pyrene bioaccessibility when spiking 3.0 and 6.0 μg
327 benzo(a)anthracene (Figure 5). Fluoranthene was spiked into the low energy FOREhST model at
328 0, 2.3, 4.5, 9.0, 18 and 36 μg, resulting in no significant difference in benzo(a)anthracene
329 bioaccessibility (Figure 5).

330 **Discussion**

331 The FOREhST model successfully predicts 66% of the variance in benzo(a)anthracene
332 and 65% of the variance in benzo(a)pyrene internal exposure across 14 soils polluted with a
333 mixture of PAHs. To our knowledge, this is the first successful application of in vitro digestor
334 results to estimate PAH bioavailability across multiple soils. We achieved this by: (i)
335 incorporating PAH-PAH interactions into the predictive algorithim, and (ii) altering the energetic
336 input of the in vitro digestors. We were led to these modifications by building on key concepts
337 outlined by Reichenberg and Mayer[13] that chemical activity, bioaccessibility and bioavailability
338 are conceptually distinct. Specifically, bioaccessibility is a combination of chemical activity and
339 solubility, and thus, human in vitro digestors should not be designed to solely estimate
340 chemical activity because factors, other than chemical activity, can influence bioaccessibility.

341 At environmentally relevant concentrations, PAH-PAH interactions can influence
342 bioaccessibility and bioavailability. Phenanthrene, pyrene, and benzo(a)pyrene were used
343 based on previous work that demonstrated the importance of this PAH-PAH interactions.[22, 23]
344 For example, Chun et al.[22], attribute the change in PAH solubility from PAH-PAH interactions to

PAH-micelle interactions. Using benzo(a)pyrene and phenanthrene in both artificial sea water and *Arenicola marina* gut fluid, Voparil et al.[23] found that phenanthrene did not significantly change the benzo(a)pyrene concentration in the artificial sea water, whereas benzo(a)pyrene concentration was increased to 154% in *Arenicola marina* gut fluid in the presence of phenanthrene, alluding to the importance of the PAH-micelle interaction. Using phenanthrene, pyrene and fluoranthene with various surfactants and water, Prak et al.[38] found that PAH-micelle interactions was a significant factor but also that PAH-PAH interactions influenced the water solubility of fluoranthene.

Typically PAH-PAH experiments are in reduced mixtures of only 1 to 3 PAHs, e.g. Chun et al.[22], Voparil et al.[23], Prak et al.[38], etc. In contrast, our dosed soils contained more than 11 PAHs. Thus, an alternate numerical method was needed to incorporate PAH-PAH interactions because we were comparing two matrices, bioaccessibility and bioavailability which contained 14 soils by 11 PAHs. Co-inertia analysis is one such method. We used co-inertia to link the matrix of PAH bioaccessibility with PAH internal exposure and identified that FOREhST release of chrysene, fluoranthene, anthracene, and benzo(a)anthracene were the principle components governing PAH uptake in vivo. For benzo(a)pyrene, we confirm that benzo(a)anthracene influences benzo(a)pyrene soil bioaccessibility. In contrast, fluoranthene does not increase benzo(a)anthracene soil bioaccessibility as predicted by statistical modelling bioaccessibility (Figure 5). Notably, PAH-PAH interactions are not limited to just desorption[39] and solubility[22, 23, 38], as PAH interactions are also relevant with cellular responses. DNA damage to HepG2 cells is modulated based on specific binary PAHs mixtures.[40] Furthermore, induction of PAH metabolizing enzymes, CYP1A1 and CYP1A2, are dependent upon exposure to specific PAHs.[41]

The collinearity of individual PAH bioavailabilities or bioaccessibilities likely reflects fundamental chemical-chemical interactions. PAHs with similar molecular weight, ring number, and structure have strong influences on each other. For example, Lui et al.[42] reports a significant correlation for PAH soil concentration of all 16 PAHs examined but a stronger correlation for PAHs of similar molecular weight. Similarly, the PAH ratio of compounds is used in PAH source appointment because ratios of similar PAHs are consistently found based on source. [20, 43] Although our results suggest the importance of chrysene, fluoranthene, benzo(a)anthracene, this may be limited to our sample set of 14 soils. In other soils, factors such as PAH source,[20, 21, 43] PAH concentration, sorption sink,[10] desorption media,[13, 14] soil physio-chemical properties,[18] dietary constituents[23], and co-contaminants[23] may further influence the partitioning dynamic of PAHs and thus, may influence the equations describing the link between in vitro bioaccessibility and in vivo internal exposure.

Energetic input through shaking method is responsible for up to 99% of PAHs released from in vitro models. PAH release from the low energy FOREhST was between 0.66% (anthracene) and 31 % (fluoranthene) with an average of 19% between PAHs compared to the high energy FOREhST. PAH kinetic desorption from soil will be dependent upon the energy of the system, both kinetic and thermal, interacting with the PAH-soil binding media, amorphous organic matter and carbonaceous geosorbents. Given the limited desorption time of the FOREhST model, ie. 4 hours, the majority of desorbed PAHs were likely bound to the rapidly desorbing amorphous organic matter as opposed to the slowly desorbing recalcitrant carbonaceous geosorbents. However, these rapidly released PAHs from amorphous geosorbents may in turn, influence PAH release from carbonaceous geosorbents. For example,

White et al.[39] observed that freshly spiked anthracene or pyrene into soil leads to increased aged phenanthrene extraction by a mild solvent and increased biodegradation, suggesting that PAHs compete for and interact at the slow desorption sites of carbonaceous geosorbents. Within the FOREhST model, it is uncertain if a similar interaction is occurring between the rapidly desorbed PAHs competing with the recalcitrant PAHs to influence bioaccessibility. If this interaction is occurring, this may explain the energetic disparity between the low and high energy FOREhST with PAH desorbed from amorphous organic matter in the high energy FOREhST increasing PAH desorption rate from the carbonaceous geosorbents. In either case the high energy FOREhST desorbs PAHs at a rate such that there is a strong correlation to soil PAH concentration, and we've repeatedly observed that soil concentration does not correlate with bioavailability.[1, 8] As a product of the desorption kinetics and desorption time of in vitro models, energetic input becomes a dominant factor linking PAH desorption from soil in an in vitro model to mammalian PAH uptake into the blood stream. Yet oddly, this factor has not been identified in the round robins of in vitro digestor performance that have been performed previously.[14, 19] Notably, the energetic input does not appear to affect all PAHs equally. In Figure 2, the high energy FOREhST does not accurately predict anthracene, fluoranthene and pyrene AUC48, wherease only fluoranthene is not predicted in the low energy FOREhST model. Suggesting that for these relatively lower molecular weight PAHs, energetic input is not a dominant factor.

When considered as single contaminants, PAH bioaccessibility and bioavailability is strongly linked to soil characteristics.[10, 44, 45] When considered as a mixture, PAH-PAH interactions dominate. Our work suggests that future work on PAH bioavailability and

411 bioaccessibility should focus on the dynamics of how the matrix of PAHs present in the soil
412 interact with mammalian systems. Such interactions should not only include the chemical
413 interactions discussed here but also the interactions of PAH mixtures with mammalian uptake
414 systems.

415 **Acknowledgements**

416 This work was supported by a NSERC Discovery Grant to SDS. This work was approved by the
417 University of Saskatchewan's Animal Research Ethics Board, and adhered to the Canadian
418 Council on Animal Care guidelines for humane animal use. Swedish soils were provided by
419 Staffan Lundstedt and Paul White. Special thanks to Philipp Mayer for scientific input.

420 **Supporting Information Available**

421 The supporting information contains five figures and six tables:

422 - The first figure is a diagram describing the low energy FOREhST method.
423 - The second figure compares low energy FOREhST bioaccessibility and soil
424 concentration for five PAHs.
425 - The third figure displays the correlation between swine area under the curve (AUC48)
426 and PAH release for both the low and high energy FOREhST models for five PAHs.
427 - The fourth figure displays phenanthrene and benzo(a)pyrene solubility in water and bile
428 fluids with mixtures consisting of one to four PAHs.
429 - The fifth figure is the output from co-inertia analysis.
430 - The sixth figure is a SEM diagram detailing the relationships between multiple predictor
431 variables of AUC48.

- The first table contains the low energy FOREhST PAH release for 11 PAHs: anthracene, fluoranthene, pyrene, benzo(a)anthracene, chrysene, benzo(b)fluoranthene, benzo(k)fluoranthene, benzo(a)pyrene, dibenzo(ah)anthracene, benzo(ghi)perylene, and indeno(123,cd)pyrene.
- The second table contains the high energy FOREhST PAH release for 11 PAHs
- The third table contains PCA output of co-inertia analysis for PAH exposure (AUC48)
- The fourth table contains the PCA output of co-inertia analysis for predictor variables of PAH exposure.
- The fifth table contains canonical weights and calculated strength of predictor variables
- The sixth table summarizes output of SEM results for benzo(a)anthracene and benzo(a)pyrene

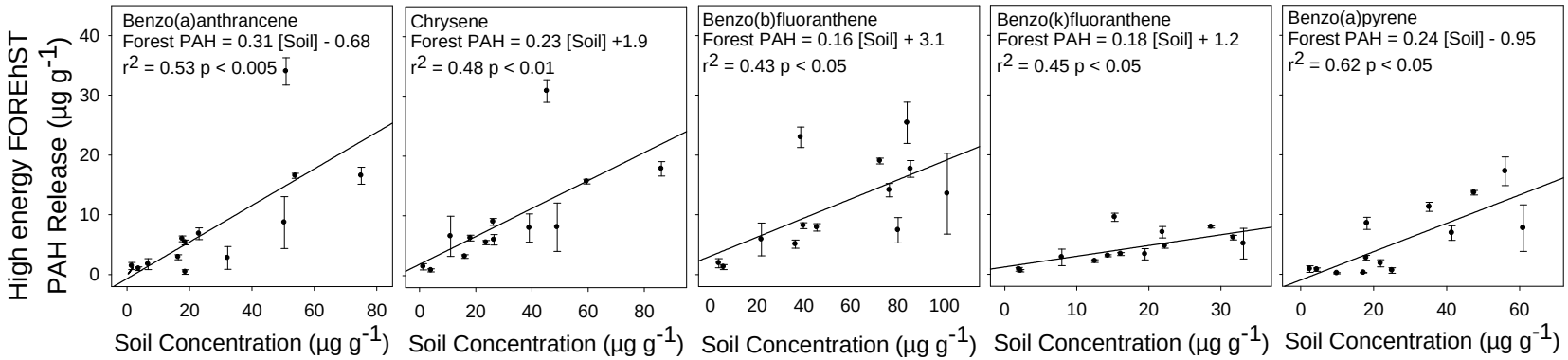

443

444 Figure 1. Comparison between FOREhST PAH release and soil concentration of five PAHs in 14 soils historically contaminated with

445 hydrocarbons. Lines indicate line of best fit. Data points represent the mean (n=3) for FOREhST PAH release and error bars

446 represent the standard error of this mean.

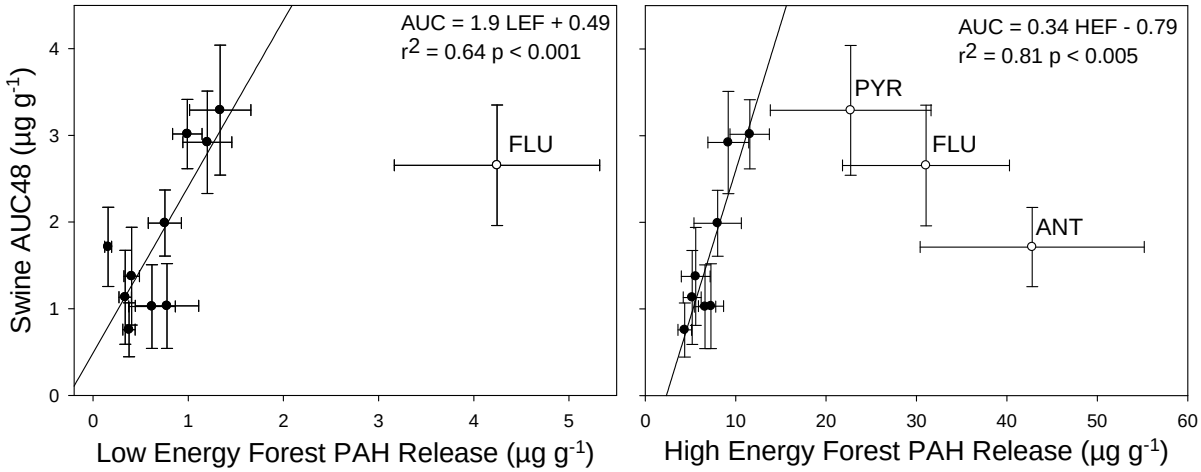

447

448 Figure 2. Regression between in vivo swine PAH area under the plasma concentration curve
449 over 48 hours in units of µg PAH recovered in plasma per gram of soil ingested (AUC48) against
450 in vitro FORE(h)ST PAH release in Low energy (left) and High energy (right). Each data point
451 represents the mean bioavailability of a single PAH from 14 soils historically contaminated with
452 PAHs and error bars are the standard error of this mean. Abbreviations are as follows: ANT is
453 anthracene, FLU is fluoranthene, PYR is pyrene.

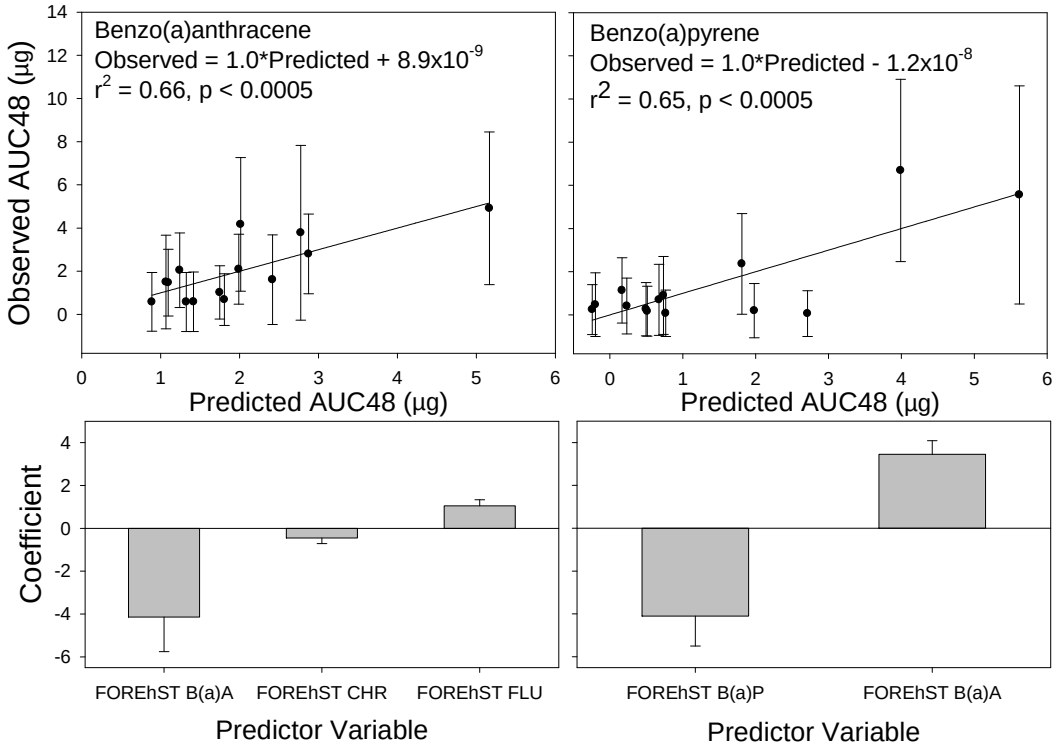

454

455 Figure 3. Comparison of observed AUC48 (area under the 48 hr plasma concentration curve)
456 versus linear model predicted AUC for benzo(a)anthracene and benzo(a)pyrene PAHs (top) and
457 the corresponding coefficient for each predictor variable (bottom). Coefficients are determined
458 using structure equation modelling. Data points for observed AUC48 represent the mean of 6
459 measurements while error bars represent the standard error of this mean. Abbreviations are
460 as follows: B(a)A is benzo(a)anthracene, CHR is chrysene, FLU is fluoranthrene, and B(a)P is
461 benzo(a)pyrene.

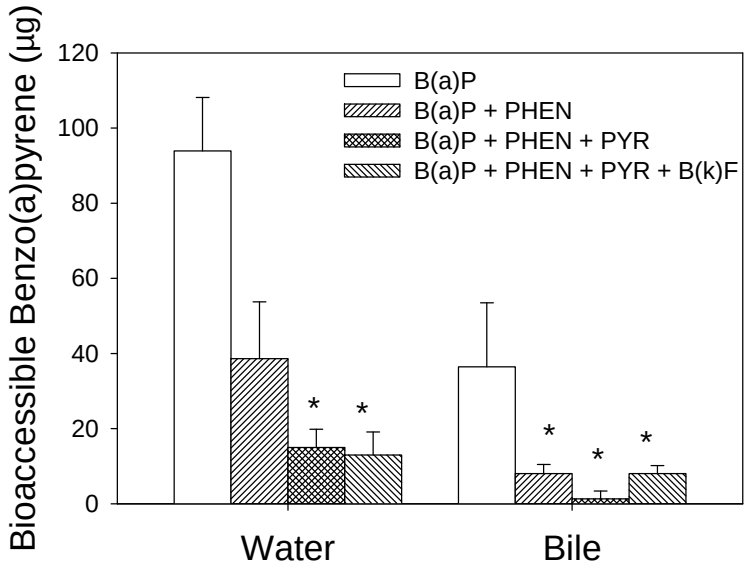

462

463 Figure 4. Bioaccessible fraction of benzo(a)pyrene in either water or bile in the presence of
464 other PAHs. Approximately 30 mg of each PAH is added to the respective treatment which is
465 above the solubility limit for the PAHs. Abbreviations are as follows: B(a)P is benzo(a)pyrene,
466 PHEN is phenanthrene, PYR is pyrene, and B(k)F is benzo(k)fluoranthene. * indicates a
467 significant ($p<0.05$) difference from bioaccessibility in the presence of only benzo(a)pyrene, i.e.
468 only benzo(a)pyrene by itself.

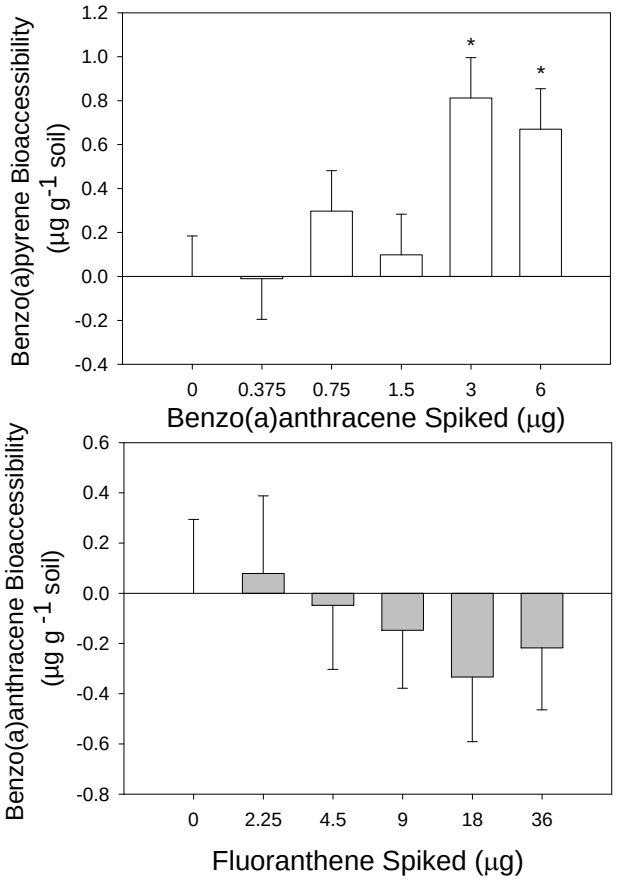

469

470 Figure 5. Top – Amount of benzo(a)pyrene released from soil in FOREhST fluids in the presence
471 of increasing amounts of benzo(a)anthracene. Bottom – Amount of benzo(a)anthracene
472 released in the presences of increasing amounts of fluoranthene. Each bar is the mean release
473 from 5 soils and error bars represent the error of this measurement with the entire experiment
474 duplicated. . '*' denotes a significant difference from acetonitrile control spike at $p < 0.05$.

475 **Table of Content Art**

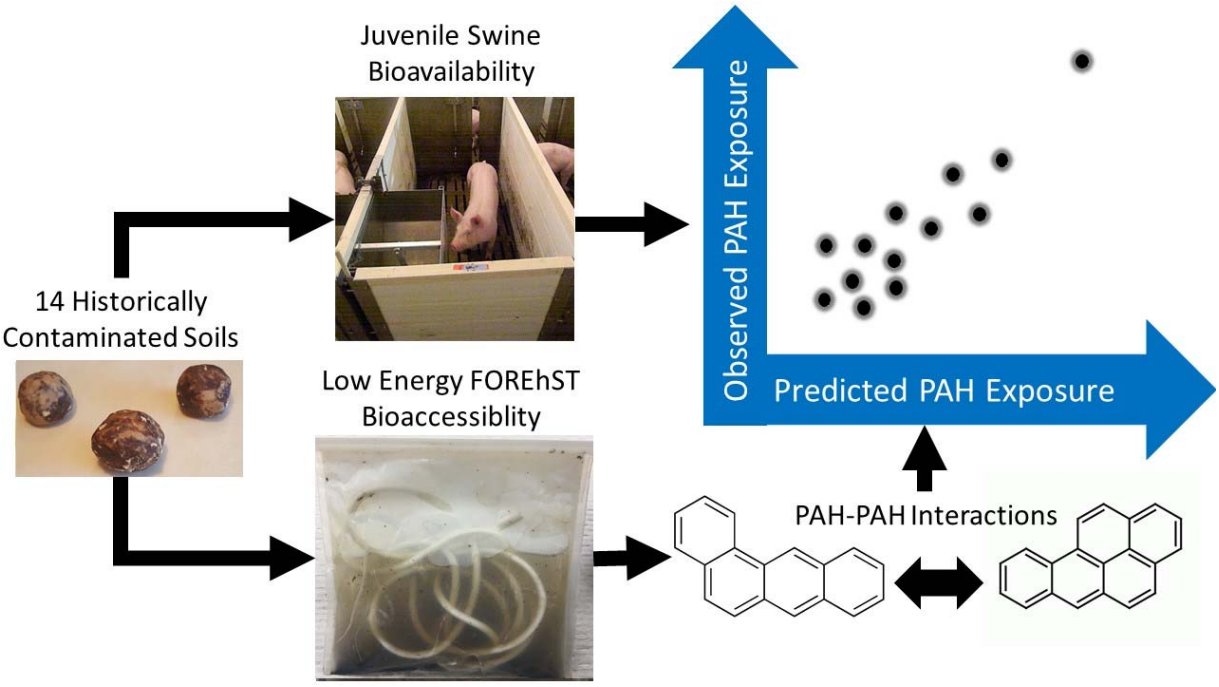

476

References

1. James, K.; Peters, R. E.; Cave, M. R.; Wickstrom, M.; Lamb, E. G.; Siciliano, S. D. Predicting Polycyclic Aromatic Hydrocarbon Bioavailability to Mammals from Incidentally Ingested Soils Using Partitioning and Fugacity. *Environ. Sci. Technol.* **2016,** *50*, (3), 1338-1346.

2. Juhasz, A. L.; Weber, J.; Stevenson, G.; Slee, D.; Gancarz, D.; Rofe, A.; Smith, E. In vivo measurement, in vitro estimation and fugacity prediction of PAH bioavailability in post-remediated creosote-contaminated soil. *Sci. Total Environ.* **2014,** *473*, 147-154.

3. Ruby, M. V.; Fehling, K. A.; Paustenbach, D. J.; Landenberger, B. D.; Holsapple, M. P. Oral bioaccessibility of dioxins/furans at low concentrations (50-350 ppt toxicity equivalent) in soil. *Environ. Sci. Technol.* **2002,** *36*, (22), 4905-4911.

4. Gouliarmou, V.; Collins, C. D.; Christiansen, E.; Mayer, P. Sorptive physiologically based extraction of contaminated solid matrices: incorporating silicone rod as absorption sink for hydrophobic organic contaminants. *Environ. Sci. Technol.* **2013,** *47*, (2), 941-8.

5. Li, C.; Cui, X. Y.; Fan, Y. Y.; Teng, Y.; Nan, Z. R.; Ma, L. Q. Tenax as sorption sink for in vitro bioaccessibility measurement of polycyclic aromatic hydrocarbons in soils. *Environ, Pollut.* **2015,** *196*, 47-52.

6. Tilston, E. L.; Gibson, G. R.; Collins, C. D. Colon Extended Physiologically Based Extraction Test (CE-PBET) Increases Bioaccessibility of Soil-Bound PAH. *Environ. Sci. Technol.***2011,** *45*, (12), 5301-5308.

7. Cave, M. R.; Wragg, J.; Harrison, I.; Vane, C. H.; Van de Wiele, T.; De Groeve, E.; Nathanail, C. P.; Ashmore, M.; Thomas, R.; Robinson, J.; Daly, P. Comparison of Batch Mode and

498 Dynamic Physiologically Based Bioaccessibility Tests for PAHs in Soil Samples. *Environ. Sci.*
499 *Technol.* **2010**, *44* (7), 2654-2660.
500 8. James, K.; Peters, R. E.; Laird, B. D.; Ma, W. K.; Wickstrom, M.; Stephenson, G. L.;
501 Siciliano, S. D. Human Exposure Assessment: A Case Study of 8 PAH Contaminated Soils Using in
502 Vitro Digestors and the Juvenile Swine Model. *Environ. Sci. Technol.* **2011,** *45*, (10), 4586-4593.
503 9. Hurdzan, C. M.; Basta, N. T.; Hatcher, P. G.; Tuovinen, O. H. Phenanthrene release from
504 natural organic matter surrogates under simulated human gastrointestinal conditions. *Ecotox*
505 *Environ Saf.* **2008**, *69* (3), 525-530.
506 10. Vasiluk, L.; Pinto, L. J.; Walji, Z. A.; Tsang, W. S.; Gobas, F.; Eickhoff, C.; Moore, M. M.
507 Benzo(a)pyrene bioavailability from pristine soil and contaminated sediment assessed using
508 two in vitro models. *Environ. Toxicol. Chem.* **2007,** *26*, (3), 387-393.
509 11. Gouliarmou, V.; Mayer, P. Sorptive Bioaccessibility Extraction (SBE) of Soils: Combining a
510 Mobilization Medium with an Absorption Sink. *Environ. Sci. Technol.***2012,** *46*, (19), 10682-
511 10689.
512 12. Juhasz, A. L.; Smith, E.; Nelson, C.; Thomas, D. J.; Bradham, K. Variability Associated with
513 As in Vivo-in Vitro Correlations When Using Different Bioaccessibility Methodologies. *Environ.*
514 *Sci. Technol.* **2014,** *48*, (19), 11646-11653.
515 13. Reichenberg, F.; Mayer, P. Two complementary sides of bioavailability: Accessibility and
516 chemical activity of organic contaminants in sediments and soils. *Environ. Toxicol. Chem.***2006,**
517 *25*, (5), 1239-1245.
518 14. Oomen, A. G.; Hack, A.; Minekus, M.; Zeijdner, E.; Cornelis, C.; Schoeters, G.; Verstraete,
519 W.; Van de Wiele, T.; Wragg, J.; Rompelberg, C. J. M.; Sips, A.; Van Wijnen, J. H. Comparison of

520 five in vitro digestion models to study the bioaccessibility of soil contaminants. *Environ. Sci.*
521 *Technol.***2002,** *36*, (15), 3326-3334.
522 15. Enell, A.; Reichenberg, F.; Ewald, G.; Warfvinge, P. Desorption kinetics studies on PAH-
523 contaminated soil under varying temperatures. *Chemosphere* **2005,** *61*, (10), 1529-1538.
524 16. Crampon, M.; Bureau, F.; Akpa-Vinceslas, M.; Bodilis, J.; Machour, N.; Le Derf, F.; Portet-
525 Koltalo, F. Correlations between PAH bioavailability, degrading bacteria, and soil characteristics
526 during PAH biodegradation in five diffusely contaminated dissimilar soils. *Environ. Sci. Pollut.*
527 *Res.* **2014,** *21*, (13), 8133-8145.
528 17. Zhang, J.; Sequaris, J. M.; Narres, H. D.; Vereecken, H.; Klumpp, E. Effect of organic
529 carbon and mineral surface on the pyrene sorption and distribution in Yangtze River sediments.
530 *Chemosphere* **2010,** *80*, (11), 1321-1327.
531 18. Cornelissen, G.; Gustafsson, O.; Bucheli, T. D.; Jonker, M. T. O.; Koelmans, A. A.; Van
532 Noort, P. C. M. Extensive sorption of organic compounds to black carbon, coal, and kerogen in
533 sediments and soils: Mechanisms and consequences for distribution, bioaccumulation, and
534 biodegradation. *Environ. Sci. Technol.* **2005**, 39, (18), 6881-6895.
535 19. Van de Wiele, T. R.; Oomen, A. G.; Wragg, J.; Cave, M.; Minekus, M.; Hack, A.; Cornelis,
536 C.; Rompelberg, C. J. M.; De Zwart, L. L.; Klinck, B.; Van Wijnen, J.; Verstraete, W.; Sips, A. J. A.
537 M. Comparison of five in vitro digestion models to in vivo experimental results: Lead
538 bioaccessibility in the human gastrointestinal tract. *J. Environ. Sci. Health, Part A: Toxic/Hazard.*
539 *Subst. Environ. Eng.* **2007,** *42*, (9), 1203-1211.
540 20. Tobiszewski, M.; Namiesnik, J. PAH diagnostic ratios for the identification of pollution
541 emission sources. *Environ. Pollut.* **2012,** *162*, 110-119.

21. Juhasz, A. L.; Tang, W.; Smith, E. Using in vitro bioaccessibility to refine estimates of human exposure to PAHs via incidental soil ingestion. *Environ. Res.* **2016,** *145*, 145-153.

22. Chun, C. L.; Lee, J. J.; Park, J. W. Solubilization of PAH mixtures by three different anionic surfactants. *Environ. Pollut.* **2002**, *118*, (3), 307-313.

23. Voparil, I. M.; Mayer, L. M.; Place, A. R. Interactions among contaminants and nutritional lipids during mobilization by digestive fluids of marine invertebrates. *Environ. Sci. Technol.***2003,** *37*, (14), 3117-3122.

24. Thioulouse, J. Simultaneous analysis of a sequence of paired ecological data tables: A comparison of several methods. *Ann. Appl. Stat.* **2011,** *5*, (4), 2300-2325.

25. Lamb, E. G.; Shirtliffe, S. J.; May, W. E. Structural equation modeling in the plant sciences: An example using yield components in oat. *Can. J. Plant. Sci.* **2011,** *91*, (4), 603-619.

26. Siciliano, S. D.; James, K.; Zhang, G. Y.; Schafer, A. N.; Peak, J. D. Adhesion and Enrichment of Metals on Human Hands from Contaminated Soil at an Arctic Urban Brownfield. *Environ. Sci. Technol.* **2009,** *43* (16), 6385-6390.

27. Versantvoort, C.; Rompelberg, C. Development and applicability of an in vitro digestion model in assessing the bioaccessibility of contaminants from food. **2004**.

28. Oomen, A. G.; Sips, A.; Groten, J. P.; Sijm, D.; Tolls, J. Mobilization of PCBs and lindane from soil during in vitro digestion and their distribution among bile salt micelles and proteins of human digestive fluid and the soil. *Environ. Sci. Technol.***2000,** *34*, (2), 297-303.

29. ATSDR. *Toxicological profile for polycyclic aromatic hydrocarbons*; Agency for Toxic Substances and Disease Registry U.S. Department of Health and Human Services: Washington DC, 1995.

564 30. Marriott, P. J.; Carpenter, P. D.; Brady, P. H.; McCormick, M. J.; Griffiths, A. J.; Hatvani, T.
565 S. G.; Rasdell, S. G. Optimization of fluorescence detection for polyaromatic hydrocarbon
566 determination by using high-performance liquid -chromatography. *J. Liq. Chromatogr.* **1993**, *16*
567 (15), 3229-3247.
568 31. R Core Team. R: A language and environment for statistical computing. R Foundation for
569 Statistical Computing: Vienna, Austria, 2013.
570 32. Dray, S.; Dufour, A. B. The ade4 package: Implementing the duality diagram for
571 ecologists. *J. Stat. Softw.* **2007,** *22*, (4), 1-20.
572 33. Doledec, S.; Chessel, D. Co-inertia anaylsis - An alternative method for studying species
573 environment relationships. *Freshw. Biol.* **1994,** *31*, (3), 277-294.
574 34. Dray, S.; Chessel, D.; Thioulouse, J. Co-inertia analysis and the linking of ecological data
575 tables. *Ecology* **2003,** *84*, (11), 3078-3089.
576 35. Venables, W. N.; Ripley, B. D. Random and mixed effects. In *Modern applied statistics*
577 *with S*. Springer: **2002**; 271-300.
578 36. Osborne, J. W.; Waters, E. Four Assumptions Of Multiple Regression That Researchers
579 Should Always Test. *Pract. Assess. Res. Eval*. **2002**, 8, (2), 1-5.
580 37. Rosseel, Y. Lavaan: An R Package for Structural Equation Modeling. *J. Stat. Softw.* **2012,**
581 *48* (2), 1-36.
582 38. Prak, D. J. L.; Pritchard, P. H. Solubilization of polycyclic aromatic hydrocarbon mixtures
583 in micellar nonionic surfactant solutions. *Water Res.* **2002,** *36*, (14), 3463-3472.

584 39. White, J. C.; Alexander, M.; Pignatello, J. J. Enhancing the bioavailability of organic
585 compounds sequestered in soil and aquifer solids. *Environ. Toxicol. Chem.* **1999,** *18*, (2), 182-
586 187.
587 40. Tarantini, A.; Maitre, A.; Lefebvre, E.; Marques, M.; Rajhi, A.; Douki, T. Polycyclic
588 aromatic hydrocarbons in binary mixtures modulate the efficiency of benzo(a)pyrene to form
589 DNA adducts in human cells. *Toxicol.* **2011,** *279*, (1-3), 36-44.
590 41. Vakharia, D. D.; Liu, N.; Pause, R.; Fasco, M.; Bessette, E.; Zhang, Q. Y.; Kaminsky, L. S.
591 Polycyclic aromatic hydrocarbon/metal mixtures: Effect on PAH induction of CYP1A1 in human
592 HEPG2 cells. *Drug Metab. Dispos.* **2001,** *29*, (7), 999-1006.
593 42. Liu, G.; Bi, R. T.; Wang, S. J.; Li, F. S.; Guo, G. L. The use of spatial autocorrelation analysis
594 to identify PAHs pollution hotspots at an industrially contaminated site. *Environ. Monit. Assess.*
595 **2013,** *185*, (11), 9549-9558.
596 43. Yunker, M. B.; Macdonald, R. W.; Vingarzan, R.; Mitchell, R. H.; Goyette, D.; Sylvestre, S.
597 PAHs in the Fraser River basin: a critical appraisal of PAH ratios as indicators of PAH source and
598 composition. *Org. Geochem.* **2002,** *33*, (4), 489-515.
599 44. Minhas, J. K.; Vasiluk, L.; Pinto, L. J.; Gobas, F.; Moore, M. M., Mobilization of chrysene
600 from soil in a model digestive system. *Environ. Toxicol. Chem.***2006,** *25*, (7), 1729-1737.
601 45. Duan, L.; Palanisami, T.; Liu, Y.; Dong, Z.; Mallavarapu, M.; Kuchel, T.; Semple, K. T.;
602 Naidu, R. Effects of ageing and soil properties on the oral bioavailability of benzo a pyrene using
603 a swine model. *Environ. Int.* **2014,** *70*, 192-202.